# OSCILLATORY, CHAOTIC AND TURBULENT THERMOCAPILLARY CONVECTIONS IN A HALF-ZONE LIQUID BRIDGE

**Hiroshi KAWAMURA[*1], Ichiro UENO[*2], Shiho TANAKA[*3]and Dai NAGANO[*4]**
Dept. Mech. Eng., Fac. Sci. & Tech., Science University of Tokyo
2641 Yamazaki, Noda-shi, Chiba 278-8510, JAPAN
*1: kawa@rs.noda.sut.ac.jp *2: ich@rs.noda.sut.ac.jp
*3: j7596401@rs.noda.sut.ac.jp *4: j7500643@rs.noda.sut.ac.jp

## ABSTRACT

Thermocapillary-driven convection in a half-zone liquid bridge was investigated experimentally. Special attention was paid upon the flow structures far beyond the critical condition. The authors categorized the induced flows into several regimes mainly by the suspended particle motion in the bridge and the surface temperature variation. Chaotic and turbulent flows were realized in this configuration. They were distinguished by applying the pseudo-phase-space reconstruction from the time series of the surface temperature.

## INTRODUCTION

The floating-zone method is a way to produce a higher-quality single crystal avoiding any contact with a vessel wall to minimize the ingression of impurity. In this method, a liquid column is formed between two solid material rods by heating the central part while cooling the both ends. Such melting and solidification processes impose inevitably a temperature gradient along the liquid column surface. As the result, the thermocapillary convection is induced from the hot center to cold ends over the molten material surface. The quality of the produced single crystal is significantly affected by the regime of the developed flow. Experimental and numerical works thus has been widely conducted to comprehensive understanding of the flow structure in the liquid column. As the fundamental research, the half-zone (HZ) method has been applied. In this method, a liquid is suspended between hot and cold rods; that is, only the half of the floating-zone method is mimicked. The thermocapillary flow develops from the hotter to colder ends. This configuration is often preferred in the fundamental research because the temperature difference can be more accurately defined. In the present study the authors focused upon the flow structure in the HZ liquid bridge.

The intensity of the flow induced by the thermocapillary force can be described by using two non-dimensional numbers of the Marangoni number $Ma$ and Prandtl number $Pr$ defined as follows;

$$Ma = \frac{\sigma_T \Delta T \cdot H}{\rho \nu \kappa}, \quad Pr = \frac{\nu}{\kappa}$$

where $\Delta T$ is the temperature difference between the both end surfaces, $\sigma_T$ the temperature coefficient of the surface tension, $H$ the height of the liquid bridge, $\rho$ the density, $\nu$ the kinematic viscosity and $\kappa$ the thermal diffusivity. In case the temperature difference between the two rods is small, the induced flow is steady and axisymmetric. When $\Delta T$ exceeds a critical value $\Delta T_c$ or $Ma \geq Ma_c$, a time-dependent non-axisymmetric flow takes place. After the onset of the time-dependent flow, modal oscillatory structures emerge in the liquid bridge. A great number of terrestrial experiments[1]-[4] have been conducted in the last three decades concerning the transition and successive modal structures of the flow field. The preceding works, however, mainly focused upon the flow structures at certain region close to the critical point of the transition. Little information has been obtained regarding the flow fields far beyond the critical point. The present study focused its attention upon the flow structures with up to a very large temperature difference to realize chaotic and turbulent flows induced by the thermocapillary force in the HZ liquid bridge. In order to distinguish the induced flow regimes a reconstruction of the pseudo-phase space from the time series of the surface-temperature signal was employed as well as the visualization of the flow field and the Fourier analysis of the temperature variation.

## EXPERIMENT

The test section is described in Fig. 1. Silicone oil of 1, 2 and 5 cSt (at 25 °C) was employed as the test fluid. Their Prandtl numbers were 16.0, 28.1 and 68.4 at 25 °C, respectively. A liquid bridge of silicone oil with small particles was formed between two cylindrical rods.

Three sets of hot and cold rods of 2, 5 and 7 mm in end-surface diameter were employed. The aspect ratio $Ar$ (= $H$ / $D$) was varied from 0.15 to 1.20, where $H$ and $D$ are the height and the diameter of the bridge, respectively. The volume ratio of the bridge was kept constant at very close to unity. The top rod was made of sapphire, which enabled us to observe the flow field in the bridge from the top end surface. The bottom one was made of aluminum whose sidewall was chemically coated to prevent wetting by the liquid. A temperature difference $\Delta T$ between the end surfaces was imposed by heating the top rod. The temperatures of the both rods were measured by thermocouples. It is noted that since the liquid bridge was heated from the top, the flow was mainly

prevailed by the thermocapillary force. The Grashof number was an order of less than a thousand. Thus, the effect of the buoyancy might exist, but must not be significant. The difference $\Delta T$ was increased up to approximately 100 K at a constant small increment of 0.1 K/s in detecting the critical condition, which was confirmed in advance to have little influence upon the critical condition for the flow-field transition.

A time series of the temperature slightly inside of the bridge at mid-height was measured with a Cr-Ar thermocouple (T/C) of 0.025 mm in diameter at sampling rates up to 50 Hz. Measured temperature was affected by the ambient air motion and resultant thermal disturbance in case the T/C was located without touching the free surface, while the thermocapillary flow field was disturbed if the junction was penetrated deeply inside of the bridge. Preliminary tests were made to determine most suitable position of the T/C junction. The position was selected to be a small depth of 0.15±0.003 mm in side the free surface, because the effect of the insertion upon the particle motion was minimal while undesirable effect of the air motion could be eliminated. With increasing $\Delta T$, the free surface expanded; so the position of T/C junction was readjusted to keep the depth constant. The temperature oscillation was detected after a waiting period of 5 minutes. The measured temperature at this location is called the surface temperature hereafter in this paper.

Several kinds of almost density-matched particles with various diameters up to 50 μm and various shapes were suspended in the liquid as tracers. The dispersion density of the particle was also varied. Flow field was observed by two CCD cameras; one from the top and the other from the side.

The whole apparatus was installed in a refrigerator to maintain the ambient temperature was kept at about -20 °C in order to suppressing the evaporation of fluid while attaining a large temperature difference.

## RESULTS AND DISCUSSIONS

### Definition of Flow Regimes

The flow structures can be categorized into several regimes owing to the Fourier spectrum of the surface temperature variation and the particle motion as shown in Table 1. Regime *Rg* with a higher number mainly corresponds to the structure emerging at a larger temperature difference.

The flow regime was primarily determined by the temperature difference $\Delta T$ and the aspect ratio $Ar$. It further depended upon the increasing rate of the temperature difference and its history. Some of these regimes did not appear in a certain run depending upon the experimental conditions.

The boundary between *Rg1* and *Rg2* is well-recognized as the critical point of the flow transition from 2-D steady to 3-D time-dependent flows. The Marangoni number at the critical point is usually called the critical Marangoni number $Ma_c$. This critical point was detected by the surface temperature fluctuation (see Fig. 2) as well as the particle motion in the bridge. This critical condition in terms of $Ma$ as a function of $Ar$ is given in Fig. 3. This figure indicates that the critical Marangoni number $Ma_c$ for the lower aspect ratio is practically independent of $D$ and $Ar$ with the value of $Ma_c = (1 - 2) \times 10^4$, while it slightly depends upon $Pr$ of the fluid. In this figure preceding experimental results from Velten *et al.*[3] and Musad *et al.*[4] are also plotted.

The convective flow shows modal structures in *Rg2* and *Rg3* as indicated experimentally by the preceding works[5][6], which is described in the following subsection. Existing works have mainly focused upon the regime up to *Rg3*. With increasing the temperature difference from *Rg2* and *Rg3*, the flow in the bridge once becomes disordered (*Rg4*). This *Rg4* is a transition regime and consists of the mixed structure of rotating and pulsating flows. Further increasing $\Delta T$, ordered structures again emerge as *Rg5* and *Rg6*. These regimes retain different kinds of pulsating and rotating flows, respectively. The particles suspended in the bridge exhibit unique structures in these regimes. In the regime of *Rg7*, the flow becomes apparently chaotic. The fundamental frequency is buried in the broadband noise. The flow in *Rg8* shows no distinct difference from that in *Rg7* apparently. In the reconstructed pseudo-phase space from the time series of the surface-temperature fluctuation, however, there exists an evident difference between these regimes. Detail description is conducted in the following subsections. Note that the structures beyond *Rg8* could not be observed because such a large temperature difference could not be attained in this system.

### Detail Description of Flow Regimes

#### Temperature variation and power spectrum of each flow regimes

The top and side views of the typical flow structures, the corresponding temperature variations and its Fourier spectra in the case of $Ar = 0.32$ are shown in Fig. 4. Note that the flow field exhibited a modal structure with a mode number $m = 3$ at around this $Ar$ after the onset of the oscillatory flow. Detail experimental conditions are shown below each picture.

Figure 4-(a)-(1) indicates the visualized flow field with a small temperature difference. At a lower $\Delta T$ than the critical value $\Delta T_c$, that is, in *Rg1*, the flow exhibits 2-D steady convection. The particles disperse in the vicinity of the free surface but never show any ordered morphological structure in the bridge.

Certain polygonal modal structures are observed from the top end surface through the visualization with the suspended particles in the fluid in *Rg2* and *Rg3* after the onset of the oscillatory flow. The tiny particles disperse in the region between the free

surface and the boundary of the polygonal region, and never penetrate into the polygonal region once the modal structure is established especially in *Rg3*. At the early stage of the oscillation the modal structure first exhibits a pulsating or standing-wave type state (*Rg2*). Figure 4-(b)-(1) shows a snapshot of *Rg2* flow. This picture indicates the transient phase between the fully developed triangle shape. The surface temperature variation of this regime *Rg2* consists of the fundamental and its harmonic frequencies (Fig. 4-(b)-(3)). The fundamental frequency is about 2 Hz, which corresponds with the frequency of the pulsating motion of the triangle. With increasing $\Delta T$, the polygonal region in the bridge then starts to azimuthally rotate (*Rg3*), although the movement of each particle stays almost radial. The direction of rotation is unable to be predicted. Figure 4-(c)-(1) shows the snapshot of the flow in *Rg3*. The periodic fluctuation of the temperature corresponding to the modal structure rotation is observed. The surface-temperature variation of *Rg3* is quite similar to that of *Rg2*. The distribution of higher frequencies than the fundamental one, however, is different from that in *Rg2*. It is noted that the surface temperature oscillates with lower fundamental frequency in *Rg3* than that in *Rg2*, in spite of the higher *Ma*. The critical condition and the successive modal structures are reported in more detail in Ref.[6]

Further increasing $\Delta T$, a distinct modal structure disappears and the particles disperse again into the whole bridge (*Rg4*). The visualized flow field seems to consist of randomly mixed structure of pulsating and rotating convection. A high-frequency fluctuation appears in the surface temperature variation, while a main frequency still remains as shown in Figs. 4-(d)-(2) and -(3). This regime *Rg4* is thus considered as a transition region of the flow structures between the first (*Rg2+Rg3*) and the second (*Rg5+Rg6*) pairs of pulsating and rotating oscillatory flows.

Beyond the transition regime *Rg4*, ordered structures again emerge as *Rg5* and *Rg6*. In *Rg5*, another standing-wave type of oscillation emerges as shown in Fig. 4-(e)-(1). The dynamic motion of the suspended particles is quite different from that in the first pulsating flow. The particles are trapped within the 1/6 azimuthally-divided cells and seldom move to the neighboring one. The temperature fluctuation in this regime (Fig. 4-(e)-(2)) is also different from that in *Rg2*. It involves an additional slope between the peaks in a basic temperature variation. The harmonics of higher order are thus seen in the spectrum.

With increasing $\Delta T$, another rotating oscillatory flow or traveling-wave type of oscillation emerges as *Rg6*. In this regime the particles accumulate along a single closed path (see Fig. 4-(f)-(1)) named as the twisted-loop particle accumulation structure (TL-PAS)[6][7]. The regime *Rg6* possesses several kinds of TL-PASs and their combined structures. Their features and three-dimensional structures are well-described by Ueno *et al.*[6] and Tanaka *et al.*[7] The fundamental frequency of *Rg6* is lower than that of *Rg5*. In addition, the spectrum indicates that the temperature fluctuation is influenced by lower frequencies than the fundamental one comparing to that of *Rg5*. Such features are also detected in the first pair of the regimes (*Rg2* and *Rg3*).

At a higher $\Delta T$, the chaotic structure emerges in the bridge. The distinct particle accumulation structure disappears and the particles disperse in the whole bridge again (Fig. 4-(g)-(1)). The surface-temperature variation apparently retains almost no periodic nature. Its power spectrum becomes rather broadened. The peaks are almost buried in the continuous frequency spectrum and hard to be distinguished. This is exactly one of the features characterizing the 'chaotic' motion. That is, the broadband fluctuation emerges intermittently and then it prevails gradually the whole space and time.

Further increasing $\Delta T$, the flow field exhibits a transition into the turbulent-like regime. It is quite difficult to distinguish the difference between *Rg7* and *Rg8* by the particle motion, the temperature variation and its Fourier spectrum. In order to categorize the flow regime in the bridge the reconstruction of the pseudo-phase space from the time series of the temperature variation is employed described as follows.

## Reconstruction of phase space

Frank and Schwabe[8] examined their experimental results by reconstructing 2-D phase space from surface-temperature time series by azimuthally located three different thermocouples to show the transition to chaotic state. In their experiments, however, the temperature signals involved the ambient-gas temperature fluctuation as well because the thermocouples were located near the surface without touching it. It is confirmed in advance by the present authors that a fundamental frequency and its harmonics of the temperature fluctuation of the fluid itself are buried under the ambient fluid temperature fluctuations. In this study a pseudo-phase-space (PPS) reconstruction is conducted from a single time series of the surface temperature by applying the time-delayed coordinates.

Figures 5-(a) to 5-(g) indicate the typical reconstructed pseudo-phase spaces of the flow fields *Rg2* to *Rg8*. The reconstruction is carried out in a fully developed state of each regime and is conducted by use of a constant time delay of $\tau = 0.1$ s. Each trajectory shown in these figures consists of 2000 detected points. Note that the axis scale is adjusted to obtain an almost equal envelope size of the trajectories. The first pair of pulsating and rotating flows exhibits weakly nonlinear periodic orbits as shown in Figs. 5-(a) and -(b). The attractor of the *Rg3* becomes more folded than that of *Rg2*. In the transition regime *Rg4*, another frequency in addition

to the fundamental one in *Rg2* and *Rg3* appears (see Fig. 4-(f)-(3)) and the trajectory is stretched and folded as shown in Fig. 5-(c). The width of the trajectory band is broadened compared with those of *Rg2*, *Rg3*, *Rg5* and *Rg6*. The structure of the trajectory shows the mixed form of that of *Rg3* and *Rg5*. It should be noted that the trajectory has a closed structure. That means the flow in *Rg4* is still essentially periodic although a definite flow structure cannot be observed. In the second pair of pulsating and rotating flows (*Rg5* and *Rg6*, respectively), the modal flow structures exist again as aforementioned. Their attractors exhibit more folded shape than those of the first pair (see Figs. 5-(a) and -(b)). In addition, more folded region appears in the orbit of *Rg6* than that of *Rg5*. This tendency is qualitatively the same in the relation between *Rg2* and *Rg3*.

Further increasing $\Delta T$ or *Ma* the ordered structure disappears as shown in Figs. 4-(g)-(1), and -(h)-(1). Although almost no distinct difference is observed in the power spectrum from the time series of temperature variations (see Figs. 4-(g)-(3) and -(h)-(3)), an evident difference is indicated in the reconstructed PPS between the *Rg7* and *Rg8* as shown in Fig. 5-(f) and -(g), respectively. In the *Rg7* the trajectory scatters and does not form a sharp and definite route, but still retains a certain structure in the PPS. At higher *Ma*, in *Rg8*, the trajectory exhibits no ordered structure. This indicates that no periodic structure exists and thus the flow exhibits the transition to the turbulent state. This is, to the best of the authors' knowledge, the first attempt that the turbulent flow has been realized in the laboratory experiments with this configuration.

## CONCLUDING REMARKS

The thermocapillary-driven flow in a half-zone liquid bridge was studied far beyond the critical point. The convection regimes from the steady to the turbulent flows were categorized by the observation of the suspended particle motion, the surface temperature variation, its Fourier spectrum and trajectory in the reconstructed pseudo-phase space.

With increasing the temperature difference $\Delta T$, the flow field exhibited a transition from 2-D steady to 3-D oscillatory flows. After the onset of the oscillation, pulsating and then rotating flows emerged. After exhibiting a transition regime, the pulsating and rotating flows were observed again, although their flow structures were quite different from the former ones. These flow regimes retained quasi-periodic structures. Further increasing the temperature difference from the second rotating flow, chaotic and turbulent states were realized in the bridge.

## ACKNOWLEDGEMENTS

The authors would like to express their thanks to Mr. Yoshihisa ONO and Mr. Kohei NISHIHATA at Science University of Tokyo for their dedicated contributions in carrying out the experiments and data analysis. A part of this work was financially supported by Grant-in-Aid from the Ministry of Education, Culture, Sports, Science and Technology.

## NOMENCLATURES

$Ar$ aspect ratio ( = $H/D$) [-]
$D$ diameter of the liquid bridge [m]
$H$ height of the liquid bridge [m]
$m$ mode number
$Rg$ flow regime
$T$ temperature [°C]
$\Delta T$ temperature difference [K]
$U_0$ characteristic velocity defined as $\sigma_T \Delta T/\rho\nu$ [m/s]

Greeks

$\kappa$ thermal diffusivity [$m^2/s$]
$\mu$ dynamic viscosity [Pa·s]
$\nu$ kinematic viscosity [$m^2/s$]
$\rho$ density [$kg/m^3$]
$\sigma$ surface tension [N/m]
$\sigma_T$ temperature coefficient of surface tension $= \partial\sigma / \partial T$ [N/m·K]
$\tau$ time delay [s]

Non-dimensional numbers

$Ma$ Marangoni number = $\sigma_T \Delta T \cdot L / \rho\nu\kappa$
$Pr$ Prandtl number = $\nu / \kappa$

## REFERENCES

[1] Preisser, F., Schwabe, D. and Scharmann, A., 1983, Steady and Oscillatory Thermocapillary Convection in Liquid Columns with Free Cylindrical Surface, *J. Fluid Mech.*, Vol. 126, pp.545-567.

[2] Kamotani, Y., Ostrach, S. and Vargas, M., 1984, Oscillatory Thermocapillary Convection in a Simulated Floating-Zone Configuration, *J. Crystal Growth*, vol. 66, pp.83-90.

[3] Velten, R., Schwabe, D. and Scharmann, A., 1991, The Periodic Instability of Thermocapillary Convection in Cylindrical Liquid Bridges, *Phys. Fluids*, A3(2), pp. 267-279.

[4] Masud, J., Kamotani, Y. and Ostrach, S., 1997, Oscillatory Thermocapillary Flow in Cylindrical Columns of High Prandtl Number Fluids, *J. Thermophysics and Heat Trans.*, Vol. 11, pp. 105-111.

[5] Ono, Y., Ueno, I. and Kawamura, H., 1999, Transition and Modal Structure of Oscillatory Marangoni Convection in Liquid Bridge, *J. Jpn. Soc. Microgravity Appl.*, vol. 16, Supp., pp.96-97.

[6] Ueno, I., Ono, Y., Nagano, D., Tanaka, S. and Kawamura. H., 2000, Modal Oscillatory Structure and Dynamic Particle Accumulation in Liquid-Bridge Marangoni Convection, *Proc. of 4th KSME-JSME Thermal Eng.* Conf., Vol. 3., pp. 265-270.

[7] Tanaka, S., Ueno, I. and Kawamura, H., 2000, Dynamic Particle Accumulation Structure in Half-Zone Liquid Bridge -- Part I: Experimental Study --, *J. Jpn. Soc. Microgravity Appl.*, 17 (Supp.), pp.111-112.

[8] Frank, S. and Schwabe, D., 1997, Temporal and Spatial Elements of Thermocapillary Convection in Floating Zones, *Experiments in Fluids*, 23, pp.234-251.

Table 1 Flow regimes in the liquid bridge

| Rg | *Rg1* | *Rg2* | *Rg3* | *Rg4* | *Rg5* | *Rg6* | *Rg7* | *Rg8* |
|---|---|---|---|---|---|---|---|---|
| Status | Steady | Pulsating I | Rotating I | Transition | Pulsating II | Rotating II | Chaotic | Turbulent-like |

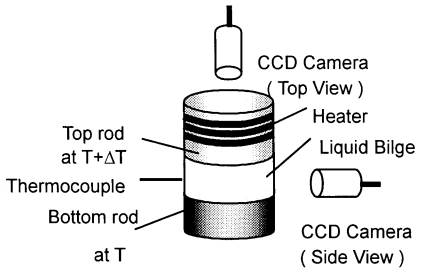


Fig.1 Experimental arrangement

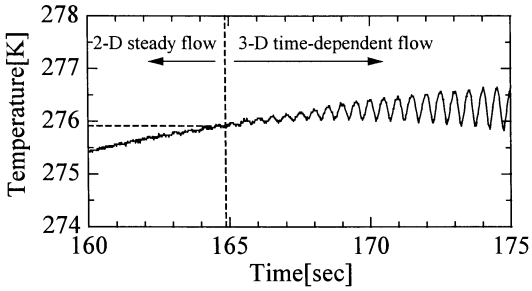


Figure 2: Point of transition from 2-D steady to 3-D time-dependent flows

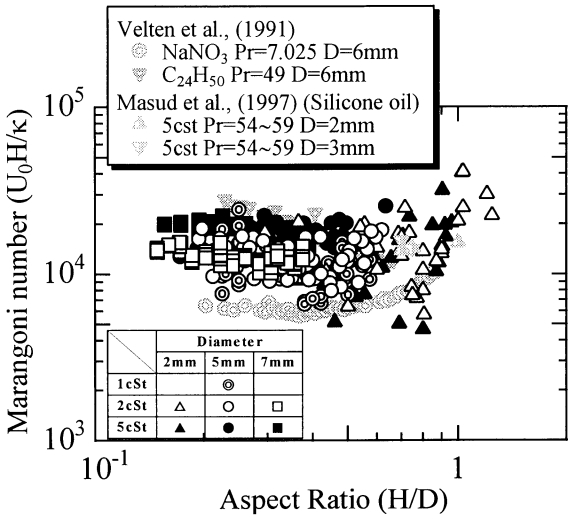


Figure 3: Critical Marangoni number for various liquid-bridge diameter,aspect ratio and Prandtl number of the fluid

(a) Rg1
Ma=26334
Δ T=28.5[K]
Ar=0.32

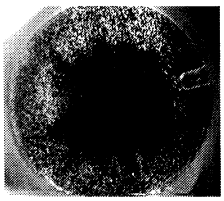

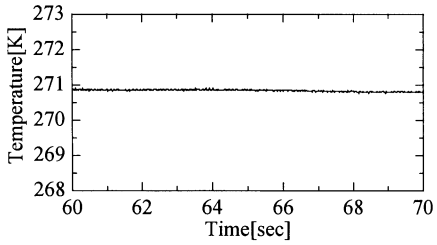


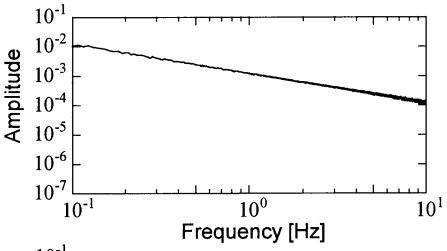


(b) Rg2
Ma=31601
Δ T=34.2[K]
Ar=0.32

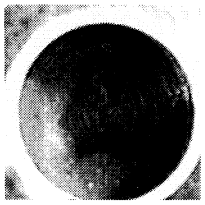

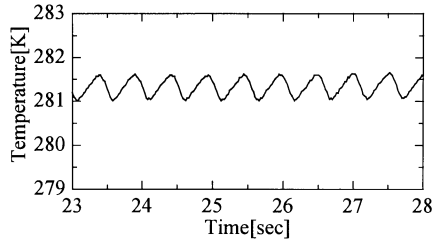


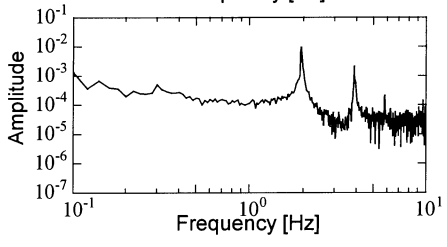


(c) Rg3
Ma=33819
Δ T=36.6[K]
Ar=0.32

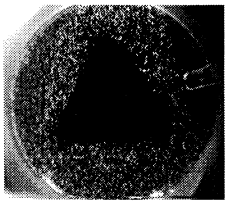

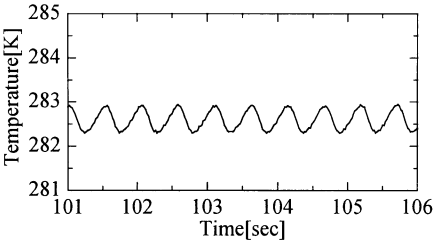


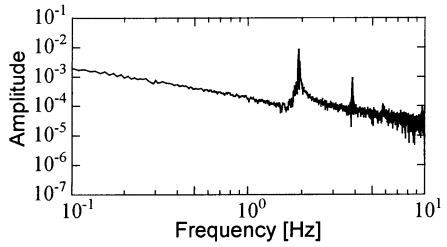


(d) Rg4
Ma=64034
Δ T=69.7[K]
Ar=0.32

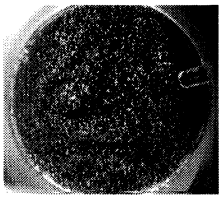

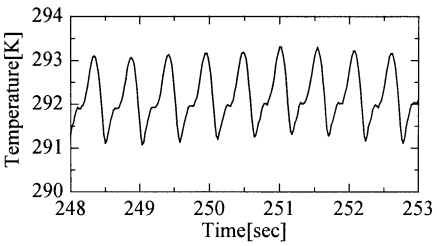


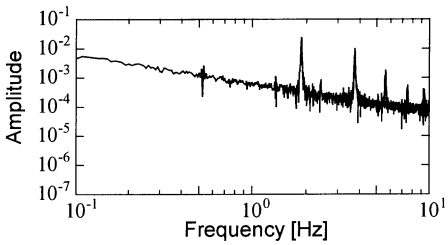

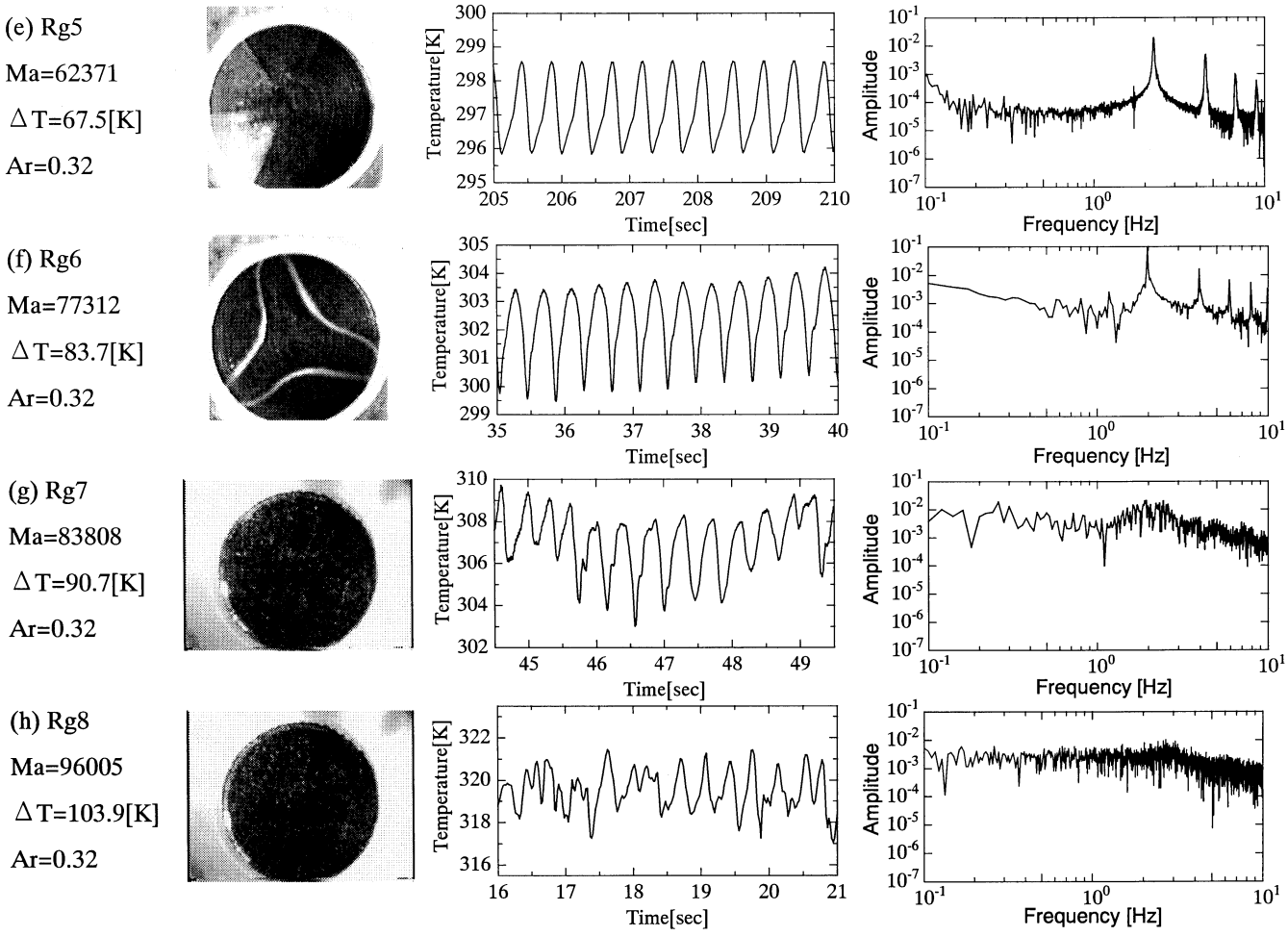


Figure 4: (1)Top views of the flow fields, (2)surface temperature variation and (3)its power spectrum density

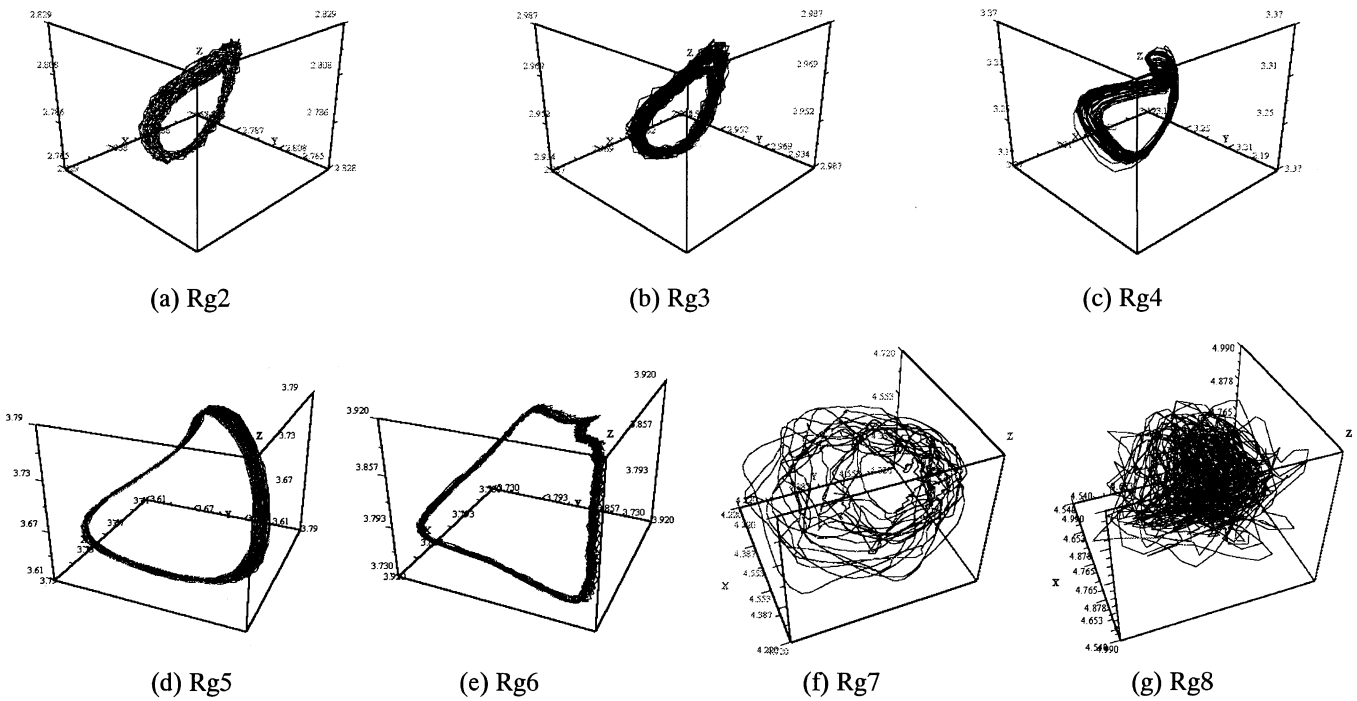


Figure 5: The trajectories in the reconstructed pseudo-phase space